Steel and Composite Structures, *Vol. 35, No. 1* (*2020*) *147-157*
DOI: https://doi.org/10.12989/scs.2020.35.1.147

Thermal buckling of nonlocal clamped exponentially graded plate according to a secant function based refined theory

Mohammed Abdulraoof Abdulrazzaq, Raad M. Fenjan, Ridha A. Ahmed and Nadhim M. Faleh*

Al-Mustansiriah University, Engineering Collage P.O. Box 46049, Bab-Muadum, Baghdad 10001, Iraq

(*Received October 17, 2019, Revised February 12, 2020, Accepted February 20, 2020*)

Abstract. In the present research, thermo-elastic buckling of small scale functionally graded material (FGM) nano-size plates with clamped edge conditions rested on an elastic substrate exposed to uniformly, linearly and non-linearly temperature distributions has been investigated employing a secant function based refined theory. Material properties of the FGM nano-size plate have exponential gradation across the plate thickness. Using Hamilton's rule and non-local elasticity of Eringen, the non-local governing equations have been stablished in the context of refined four-unknown plate theory and then solved via an analytical method which captures clamped boundary conditions. Buckling results are provided to show the effects of different thermal loadings, non-locality, gradient index, shear deformation, aspect and length-to-thickness ratios on critical buckling temperature of clamped exponential graded nano-size plates.

Keywords: thermal buckling; refined theory; exponential graded material; functionally graded material

1. Introduction

Normally, due to their specific properties, composite materials have found very wide applications in various applications into modern industrial construction such as mechanical engineering, aerospace, transportation industries and so on. However, in extreme conditions as a use in the high-temperature environments, these classical composite materials represent some deficits and fail to preserve their integrity. To surmount these drawbacks, a new sort of advanced composite materials or functionally graded materials (FGMs) have been designed. Usually these materials are made from a mixture of a ceramic and a metal with volume fractions which are varied continuously as a function of location depending on some dimension(s) of the structure to reach a required function. The FGMs have been applied in several hi-tech industrial applications of for defense industries, aerospace, aircrafts, automobile, shipbuilding industries, and further engineering structures. Presenting these notable advantages, studies of structures made of these types of materials have attracted the worldwide interest by numerous researchers (Kettaf *et al*. 2013, Zidi *et al.* 2014, Bouderba *et al*. 2013, Ait Yahia *et al.* 2015, Atmane *et al.* 2015, Mirjavadi *et al.* 2017).

New studies focus on engineering structures at nano-scales due to their involvement in nano-mechanical systems or devices. However, the main issue in these studies is to select an appropriate elasticity theory accounting for small scale impacts. The impact of size-dependency might be considered with the help of a scale parameter involved in non-local theory of elasticity (Reddy 2007, Pradhan and Phadikar 2009, Aydogdu 2009, Murmu and Adhikari 2010, Ahouel *et al.* 2016, Houari *et al.* 2018). The word "non-local" means that the stresses are not local anymore. This is because we are talking about a stress field of nano-scale structure. Many authors are aware of these facts and they are using this theory to analysis mechanical characteristics of small size engineering structures. Strain gradients at nano-scale are observed by many researchers (Alimirzaei *et al.* 2019, Chemi *et al.* 2015, Besseghier *et al*. 2015). Thus, nonlocal-strain gradient theory was introduced as a general theory which contains an additional strain gradient parameter together with nonlocal parameter (Natarajan *et al.* 2012, Cherif *et al*. 2018). The scale parameters used in nonlocal strain gradient theory can be obtained by fitting obtained theoretical results with available experimental data and even molecular dynamic (MD) simulations. Recently, it is shown that thermal loads have great impacts on static stability characteristics of small scale structures. This is due to the reason that such loads lead to reduced stiffness of the structure during the loading.

The higher-order shear deformation theories, widely known as HSDT, offer advantageous properties including consideration of various boundary conditions on the upper and lower faces (Soldatos 1992, Reddy 1984, Akvaci 2014, Mahi and Tounsi 2015, Sahoo and Singh 2013, Thai *et al*. 2014, Bourada *et al.* 2019, Boutaleb *et al.* 2019, Chaabane *et al.* 2019). Further, compaction and shear deformation effects of the core can be modeled using these theories. It should be added that other researchers employed higher-order shear deformation theories to investigate the behavior of sandwich structures with various cross-section types subjected to different loadings (El-Haina *et al.* 2017, Menasria *et al.* 2017, Mokhtar *et al.* 2018, Semmah *et al*. 2019, Tlidji *et al*. 2019, Youcef *et al.* 2018, Zarga *et al.* 2019, Mahmoudi *et al*. 2019, Draiche *et al.* 2019). In

*Corresponding author, Professor
E-mail: dr.nadhim@uomustansiriyah.edu.iq

ISSN: 1229-9367 (Print), 1598-6233 (Online)

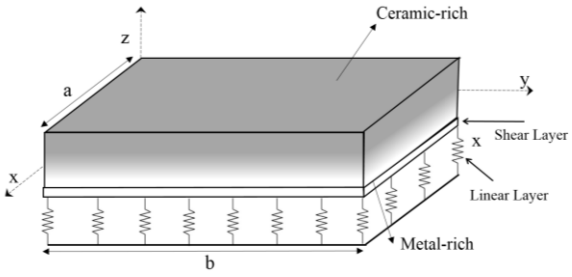

Fig. 1 A functionally graded nano-size plate rested on substrate.

addition, different types of boundary conditions were considered in these researches. A number of these studies are available in full detain in (Oktem *et al.* 2012, Mantari *et al.* 2012, Taj *et al.* 2013, Ebrahimi and Barati 2015).

Studied in this article is thermo-elastic buckling of small scale functionally graded material (FGM) nano-size plates with clamped edge conditions rested on an elastic substrate exposed to uniformly, linearly and non-linearly temperature distributions employing a secant function based refined theory. Material properties of the FGM nano-size plate have exponential gradation across the plate thickness. Using Hamilton's rule and non-local elasticity of Eringen, the non-local governing equations have been stablished in the context of refined four-unknown plate theory and then solved via an analytical method which captures clamped boundary conditions. Buckling results are provided to show the effects of different thermal loadings, non-locality, gradient index, shear deformation and length-to-thickness ratios on critical buckling temperature of clamped exponential graded nano-size plates.

2. Basic relations

2.1 Exponential functionally graded material (E-FGM) model

Suppose a FGM nano-size plate with dimensions illustrated in Fig. 1. Such FGM nano-size plate has variable material properties in transverse directions which can be defined according power-law functions of elastic modulus (*E(z)*), Poisson's ratio (ν) and thermal factor (α) as

$$E(z) = (E_c - E_m)\left(\frac{z}{h} + \frac{1}{2}\right)^p + E_m, \tag{1}$$

$$\nu(z) = (\nu_c - \nu_m)\left(\frac{z}{h} + \frac{1}{2}\right)^p + \nu_m, \tag{2}$$

$$\alpha(z) = (\alpha_c - \alpha_m)\left(\frac{z}{h} + \frac{1}{2}\right)^p + \alpha_m, \tag{3}$$

or exponentially graded model as follows (see Zenkour 2014)

$$E(z) = E_m \exp\left[\ln\left(\frac{E_c}{E_m}\right)\left(\frac{z}{h} + \frac{1}{2}\right)^p\right], \tag{4}$$

$$\nu(z) = \nu_m \exp\left[\ln\left(\frac{\nu_c}{\nu_m}\right)\left(\frac{z}{h} + \frac{1}{2}\right)^p\right], \tag{5}$$

$$\alpha(z) = \alpha_m \exp\left[\ln\left(\frac{\alpha_c}{\alpha_m}\right)\left(\frac{z}{h} + \frac{1}{2}\right)^p\right]. \tag{6}$$

in above relations, p defines the gradient exponent which states the variable material distributions in transverse direstion.

2.2 Basic relations

Modeling of the nanoplate is performed employing a 4-unknown plate theory which has fewer field unknowns compared with the refined 5-unknown and also first order plate theory (Beldjelili *et al*. 2016, Bounouara *et al*. 2016, Berghouti *et al.* 2019, Boukhlif *et al.* 2019, Boulefrakh *et al.* 2019, Abualnour *et al*. 2018, Addou *et al.* 2019, Attia *et al.* 2018). The three dimensional displacement field (u_1, u_2, u_3) of the 4-unknown plate model can be expressed by

$$\begin{aligned} u_1(x,y,z) &= u(x,y) - z\frac{\partial w_b}{\partial x} - f(z)\frac{\partial w_s}{\partial x}, \\ u_2(x,y,z) &= v(x,y) - z\frac{\partial w_b}{\partial y} - f(z)\frac{\partial w_s}{\partial y}, \\ u_3(x,y,z) &= w_b(x,y) + w_s(x,y), \end{aligned} \tag{7}$$

Here, *u* and *v* are in-plane displacements and *w* denotes the transverse displacement; $f(z)$ is shear deformation function.

$$f(z) = z - z\sec\left(\frac{rz}{h}\right) + z\sec\left(\frac{r}{2}\right)\left[1 + \frac{r}{2}\tan\left(\frac{r}{2}\right)\right], \tag{8}$$

in which $r = 0.1$. Finally, the strains based on the 4-unknown plate model are obtained as

$$\begin{aligned} \begin{Bmatrix} \varepsilon_x \\ \varepsilon_y \\ \gamma_{xy} \end{Bmatrix} &= \begin{Bmatrix} \varepsilon_x^0 \\ \varepsilon_y^0 \\ \gamma_{xy}^0 \end{Bmatrix} + z\begin{Bmatrix} \kappa_x^b \\ \kappa_y^b \\ \kappa_{xy}^b \end{Bmatrix} + f(z)\begin{Bmatrix} \kappa_x^s \\ \kappa_y^s \\ \kappa_{xy}^s \end{Bmatrix}, \qquad \begin{Bmatrix} \gamma_{yz} \\ \gamma_{xz} \end{Bmatrix} \\ &= g(z)\begin{Bmatrix} \gamma_{yz}^s \\ \gamma_{xz}^s \end{Bmatrix}, \end{aligned} \tag{9}$$

where $g(z) = 1 - f'(z)$ and

$$\begin{Bmatrix} \varepsilon_x^0 \\ \varepsilon_y^0 \\ \gamma_{xy}^0 \end{Bmatrix} = \begin{Bmatrix} \frac{\partial u}{\partial x} \\ \frac{\partial v}{\partial y} \\ \frac{\partial u}{\partial y} + \frac{\partial v}{\partial x} \end{Bmatrix}, \quad \begin{Bmatrix} \kappa_x^b \\ \kappa_y^b \\ \kappa_{xy}^b \end{Bmatrix} = -\begin{Bmatrix} \frac{\partial^2 w_b}{\partial x^2} \\ \frac{\partial^2 w_b}{\partial y^2} \\ 2\frac{\partial^2 w_b}{\partial x \partial y} \end{Bmatrix}, \quad \begin{Bmatrix} \kappa_x^s \\ \kappa_y^s \\ \kappa_{xy}^s \end{Bmatrix} = -\begin{Bmatrix} \frac{\partial^2 w_s}{\partial x^2} \\ \frac{\partial^2 w_s}{\partial y^2} \\ 2\frac{\partial^2 w_s}{\partial x \partial y} \end{Bmatrix}, \quad \begin{Bmatrix} \gamma_{yz}^s \\ \gamma_{xz}^s \end{Bmatrix} = \begin{Bmatrix} \frac{\partial w_s}{\partial y} \\ \frac{\partial w_s}{\partial x} \end{Bmatrix}. \tag{10}$$

The non-local governing equations may be derived based upon Hamilton's rule which is defined by

$$\int_0^t \delta(U+V)\mathrm{d}t = 0. \tag{11}$$

Here U and V are energies due to internal and external forces. However, internal energy variation may be determined as

$$\begin{aligned}\delta U &= \iiint_{\mathrm{v}} \sigma_{ij}\delta\varepsilon_{ij}\mathrm{dv} \\ &= \iiint_{\mathrm{v}} \left(\sigma_x\delta\varepsilon_x + \sigma_y\delta\varepsilon_y + \sigma_{yz}\delta\gamma_{yz} + \sigma_{xz}\delta\gamma_{xz} \right. \\ &\qquad \left. + \sigma_{xy}\delta\gamma_{xy}\right)\mathrm{dv}.\end{aligned} \tag{12}$$

Placing Eqs. (9) and (10) into Eq. (12) gives

$$\begin{aligned}\delta U = \iint_A \Big[& N_x\frac{\partial\delta u}{\partial x} - M_x^b\frac{\partial^2\delta w_b}{\partial x^2} - M_x^s\frac{\partial^2\delta w_s}{\partial x^2} \\ & + N_y\frac{\partial\delta v}{\partial y} - M_y^b\frac{\partial^2\delta w_b}{\partial y^2} - M_y^s\frac{\partial^2\delta w_s}{\partial y^2} \\ & + N_{xy}\left(\frac{\partial\delta u}{\partial y} + \frac{\partial\delta v}{\partial x}\right) - 2M_{xy}^b\frac{\partial^2\delta w_b}{\partial x\partial y} - \\ & 2M_{xy}^s\frac{\partial^2\delta w_s}{\partial x\partial y} + Q_{yz}\frac{\partial\delta w_s}{\partial y} + Q_{xz}\frac{\partial\delta w_s}{\partial x}\Big]\mathrm{d}A,\end{aligned} \tag{13}$$

so that forces and moments may be defined based on below relations

$$\begin{aligned}\{N_i, M_i^b, M_i^s\} &= \int_{-\frac{h}{2}}^{\frac{h}{2}} \{1, z, f\}\sigma_i\mathrm{d}z\,, \qquad i = (x, y, xy), \\ Q_j &= \int_{-h/2}^{h/2} g\sigma_j\mathrm{d}z\,, \qquad j = (xz, yz).\end{aligned} \tag{14}$$

Also, external energy variation may be determined as

$$\begin{aligned}\delta V = \iint_A \Big[& N_x^0\frac{\partial(w_b+w_s)}{\partial x}\frac{\partial\delta(w_b+w_s)}{\partial x} \\ & + N_y^0\frac{\partial(w_b+w_s)}{\partial y}\frac{\partial\delta(w_b+w_s)}{\partial y} \\ & + 2\delta N_{xy}^0\frac{\partial(w_b+w_s)}{\partial x}\frac{\partial(w_b+w_s)}{\partial y} \\ & - k_W\delta(w_b+w_s) \\ & + k_P\nabla^2\delta(w_b+w_s)\Big]\mathrm{d}A,\end{aligned} \tag{15}$$

where ∇^2 is the Laplacian, N_x^0, N_y^0 and N_{xy}^0 are in-plane forces and k_W and k_P are elastic substrate parameters. By inserting Eqs. (12) and (14) into Eq. (11) and considering the coefficients of δu, δv, δw_b and δw_s as zero, the below governing equations may be derived

$$\frac{\partial N_x}{\partial x} + \frac{\partial N_{xy}}{\partial y} = 0, \tag{16}$$

$$\frac{\partial N_{xy}}{\partial x} + \frac{\partial N_y}{\partial y} = 0, \tag{17}$$

$$\frac{\partial^2 M_x^b}{\partial x^2} + 2\frac{\partial^2 M_{xy}^b}{\partial x\partial y} + \frac{\partial^2 M_y^b}{\partial y^2} - k_W(w_b+w_s) + \tag{18}$$

$$\begin{aligned}&(k_P - N^T)\nabla^2(w_b+w_s) = 0, \\ &\frac{\partial^2 M_x^s}{\partial x^2} + 2\frac{\partial^2 M_{xy}^s}{\partial x\partial y} + \frac{\partial^2 M_y^s}{\partial y^2} + \frac{\partial Q_{xz}}{\partial x} + \frac{\partial Q_{yz}}{\partial y} \\ &\qquad - k_W(w_b+w_s) \\ &\qquad + (k_P - N^T)\nabla^2(w_b+w_s) = 0.\end{aligned} \tag{19}$$

It is supposed that the nano-size plate is exposed to a bi-axial thermal loads and the shear loads have been discarded ($N_x^0 = N_y^0 = N^T$, $N_{xy}^0 = 0$). So, thermal resultant can be defined as

$$N^T = \int_{-h/2}^{h/2} \frac{E(z,T)}{1-\nu(z)}\alpha(z,T)(T-T_0)\mathrm{d}z. \tag{20}$$

2.3 The non-local elasticity model for FG nanoplate

In the context of Eringen's non-local elasticity model (Eringen and Edelen 1972), the stress situation at every point within a structure is a function of strains of all points in the neighbor zones. Therefore, the non-local stress tensor at point x in the solid can be stated by (Fenjan *et al*. 2019, Al-Maliki *et al.* 2019)

$$\sigma_{ij}(x) = \iiint_{\Omega} \varrho(|x'-x|,\tau)t_{ij}(x')\mathrm{d}\Omega(x'), \tag{21}$$

where $t_{ij}(x')$ denotes the local stress tensor and is associated with the strain tensor based on below relation

$$t_{ij} = C_{ijkl}\varepsilon_{kl}. \tag{22}$$

Also, the nonlocal kernel $\varrho(|x'-x|,\tau)$ enumerates the influence of strains at point x' on the stresses at the point x and ϱ is an internal characteristic length (e.g., lattice parameter, granular distance, the length of C-C bonds). In addition, $\tau = e_0a/l$ is a constant which depends on the internal and external characteristic length (e.g., crack length and wavelength). Finally, non-local constitutive relations for the present FG nanoplate may be expressed by

$$\begin{aligned}&(1-\mu\nabla^2)\begin{Bmatrix}\sigma_x\\ \sigma_y\\ \sigma_{yz}\\ \sigma_{xz}\\ \sigma_{xy}\end{Bmatrix} \\ &= \begin{bmatrix}Q_{11} & Q_{12} & 0 & 0 & 0\\ Q_{12} & Q_{22} & 0 & 0 & 0\\ 0 & 0 & Q_{44} & 0 & 0\\ 0 & 0 & 0 & Q_{55} & 0\\ 0 & 0 & 0 & 0 & Q_{66}\end{bmatrix}\begin{Bmatrix}\varepsilon_x - \alpha\Delta T\\ \varepsilon_y - \alpha\Delta T\\ \gamma_{yz}\\ \gamma_{xz}\\ \gamma_{xy}\end{Bmatrix},\end{aligned} \tag{23}$$

where $\mu = (e_0a)^2$ and

$$\begin{aligned}Q_{11} = Q_{22} &= \frac{E(z)}{1-\nu^2(z)}, \qquad Q_{12} \\ &= \nu(z)Q_{11}, \qquad Q_{44} = Q_{55} \\ &= Q_{66} = \frac{E(z)}{2[1+\nu(z)]}.\end{aligned} \tag{24}$$

After integrating Eq. (22) in thickness direction, we get to the following relationships

$$(1-\mu\nabla^2)\begin{Bmatrix}N_x\\N_y\\N_{xy}\end{Bmatrix}=\begin{bmatrix}A_{11}&A_{12}&0\\A_{12}&A_{22}&0\\0&0&A_{66}\end{bmatrix}\begin{Bmatrix}\dfrac{\partial u}{\partial x}\\\dfrac{\partial v}{\partial y}\\\dfrac{\partial u}{\partial y}+\dfrac{\partial v}{\partial x}\end{Bmatrix} -\begin{bmatrix}B_{11}&B_{12}&0\\B_{12}&B_{22}&0\\0&0&B_{66}\end{bmatrix}\begin{Bmatrix}\dfrac{\partial^2 w_b}{\partial x^2}\\\dfrac{\partial^2 w_b}{\partial y^2}\\2\dfrac{\partial^2 w_b}{\partial x\partial y}\end{Bmatrix} -\begin{bmatrix}B_{11}^s&B_{12}^s&0\\B_{12}^s&B_{22}^s&0\\0&0&B_{66}^s\end{bmatrix}\begin{Bmatrix}\dfrac{\partial^2 w_s}{\partial x^2}\\\dfrac{\partial^2 w_s}{\partial y^2}\\2\dfrac{\partial^2 w_s}{\partial x\partial y}\end{Bmatrix}-\begin{Bmatrix}N_x^T\\N_y^T\\0\end{Bmatrix} \tag{25}$$

$$(1-\mu\nabla^2)\begin{Bmatrix}M_x^b\\M_y^b\\M_{xy}^b\end{Bmatrix}=\begin{bmatrix}B_{11}&B_{12}&0\\B_{12}&B_{22}&0\\0&0&B_{66}\end{bmatrix}\begin{Bmatrix}\dfrac{\partial u}{\partial x}\\\dfrac{\partial v}{\partial y}\\\dfrac{\partial u}{\partial y}+\dfrac{\partial v}{\partial x}\end{Bmatrix} -\begin{bmatrix}D_{11}&D_{12}&0\\D_{12}&D_{22}&0\\0&0&D_{66}\end{bmatrix}\begin{Bmatrix}\dfrac{\partial^2 w_b}{\partial x^2}\\\dfrac{\partial^2 w_b}{\partial y^2}\\2\dfrac{\partial^2 w_b}{\partial x\partial y}\end{Bmatrix} -\begin{bmatrix}D_{11}^s&D_{12}^s&0\\D_{12}^s&D_{22}^s&0\\0&0&D_{66}^s\end{bmatrix}\begin{Bmatrix}\dfrac{\partial^2 w_s}{\partial x^2}\\\dfrac{\partial^2 w_s}{\partial y^2}\\2\dfrac{\partial^2 w_s}{\partial x\partial y}\end{Bmatrix}-\begin{Bmatrix}M_x^{bT}\\M_y^{bT}\\0\end{Bmatrix}, \tag{26}$$

$$(1-\mu\nabla^2)\begin{Bmatrix}M_x^s\\M_y^s\\M_{xy}^s\end{Bmatrix}=\begin{bmatrix}B_{11}^s&B_{12}^s&0\\B_{12}^s&B_{22}^s&0\\0&0&B_{66}^s\end{bmatrix}\begin{Bmatrix}\dfrac{\partial u}{\partial x}\\\dfrac{\partial v}{\partial y}\\\dfrac{\partial u}{\partial y}+\dfrac{\partial v}{\partial x}\end{Bmatrix} -\begin{bmatrix}D_{11}^s&D_{12}^s&0\\D_{12}^s&D_{22}^s&0\\0&0&D_{66}^s\end{bmatrix}\begin{Bmatrix}\dfrac{\partial^2 w_b}{\partial x^2}\\\dfrac{\partial^2 w_b}{\partial y^2}\\2\dfrac{\partial^2 w_b}{\partial x\partial y}\end{Bmatrix} -\begin{bmatrix}H_{11}^s&H_{12}^s&0\\H_{12}^s&H_{22}^s&0\\0&0&H_{66}^s\end{bmatrix}\begin{Bmatrix}\frac{\partial^2 w_s}{\partial x^2}\\\frac{\partial^2 w_s}{\partial y^2}\\2\frac{\partial^2 w_s}{\partial x\partial y}\end{Bmatrix}-\begin{Bmatrix}M_x^{sT}\\M_y^{sT}\\0\end{Bmatrix}, \tag{27}$$

$$(1-\mu\nabla^2)\begin{Bmatrix}Q_y\\Q_x\end{Bmatrix}=\begin{bmatrix}A_{44}^s&0\\0&A_{55}^s\end{bmatrix}\begin{Bmatrix}\dfrac{\partial w_s}{\partial y}\\\dfrac{\partial w_s}{\partial x}\end{Bmatrix}, \tag{28}$$

so that

$$\begin{Bmatrix}A_{11},B_{11},B_{11}^s,D_{11},D_{11}^s,H_{11}^s\\A_{12},B_{12},B_{12}^s,D_{12},D_{12}^s,H_{12}^s\\A_{66},B_{66},B_{66}^s,D_{66},D_{66}^s,H_{66}^s\end{Bmatrix}= \int_{-h/2}^{h/2}Q_{11}(1,z,f,z^2,zf,f^2)\begin{Bmatrix}1\\\nu(z)\\\frac{1-\nu(z)}{2}\end{Bmatrix}\mathrm{d}z, \tag{29}$$

$$A_{44}^s=A_{55}^s=\int_{-h/2}^{h/2}g^2\frac{E(z)}{2[1+\nu(z)]}\mathrm{d}z.$$

Note that A_{22}=A_{11}. Also, the stress and moment resultants $N_x^T=N_y^T$, $M_x^{bT}=M_y^{bT}$ and $M_x^{sT}=M_y^{sT}$ due to thermal loadings are defined as

$$\begin{Bmatrix}N_x^T\\M_x^{bT}\\M_x^{sT}\end{Bmatrix}=\int_{-h/2}^{h/2}\frac{E(z,T)}{1-\nu(z)}\alpha(z,T)(T-T_0)\begin{Bmatrix}1\\z\\f(z)\end{Bmatrix}\mathrm{d}z. \tag{30}$$

Four equations of motion for exponential graded plate based on non-local theory will be achieved by placing Eqs. (24)-(27) in Eqs. (15)-(18) by

$$A_{11}\frac{\partial^2 u}{\partial x^2}+A_{66}\frac{\partial^2 u}{\partial y^2}+(A_{12}+A_{66})\frac{\partial^2 v}{\partial x\partial y}-B_{11}\frac{\partial^3 w_b}{\partial x^3} -(B_{12}+2B_{66})\frac{\partial^3 w_b}{\partial x\partial y^2} -B_{11}^s\frac{\partial^3 w_s}{\partial x^3}-(B_{12}^s+2B_{66}^s)\frac{\partial^3 w_s}{\partial x\partial y^2}=0 \tag{31}$$

$$A_{66}\frac{\partial^2 v}{\partial x^2}+A_{22}\frac{\partial^2 v}{\partial y^2}+(A_{12}+A_{66})\frac{\partial^2 u}{\partial x\partial y}-B_{22}\frac{\partial^3 w_b}{\partial y^3} -(B_{12}+2B_{66})\frac{\partial^3 w_b}{\partial x^2\partial y} -B_{22}^s\frac{\partial^3 w_s}{\partial y^3}-(B_{12}^s+2B_{66}^s)\frac{\partial^3 w_s}{\partial x^2\partial y}=0 \tag{32}$$

$$B_{11}\frac{\partial^3 u}{\partial x^3}+(B_{12}+2B_{66})\left(\frac{\partial^3 u}{\partial x\partial y^2}+\frac{\partial^3 v}{\partial x^2\partial y}\right)+B_{22}\frac{\partial^3 v}{\partial y^3} -D_{11}\frac{\partial^4 w_b}{\partial x^4} -2(D_{12}+2D_{66})\frac{\partial^4 w_b}{\partial x^2\partial y^2}-D_{22}\frac{\partial^4 w_b}{\partial y^4}-D_{11}^s\frac{\partial^4 w_s}{\partial x^4} -2(D_{12}^s+2D_{66}^s)\frac{\partial^4 w_s}{\partial x^2\partial y^2} \tag{33}$$

$$-D_{22}^{s}\frac{\partial^4 w_s}{\partial y^4}-(1-\mu\nabla^2)[k_W(w_b+w_s) - (k_P-N^T)\nabla^2(w_b+w_s)]=0,$$

$$B_{11}^{s}\frac{\partial^3 u}{\partial x^3}+(B_{12}^{s}+2B_{66}^{s})\left(\frac{\partial^3 u}{\partial x\partial y^2}+\frac{\partial^3 v}{\partial x^2\partial y}\right) + B_{22}^{s}\frac{\partial^3 v}{\partial y^3}-D_{11}^{s}\frac{\partial^4 w_b}{\partial x^4}+A_{55}^{s}\frac{\partial^2 w_s}{\partial x^2} +A_{44}^{s}\frac{\partial^2 w_s}{\partial y^2}-2(D_{12}^{s}+2D_{66}^{s})\frac{\partial^4 w_b}{\partial x^2\partial y^2} - D_{22}^{s}\frac{\partial^4 w_b}{\partial y^4}-H_{11}^{s}\frac{\partial^4 w_s}{\partial x^4} - 2(H_{12}^{s}+2H_{66}^{s})\frac{\partial^4 w_s}{\partial x^2\partial y^2} \quad (34)$$

$$-H_{22}^{s}\frac{\partial^4 w_s}{\partial y^4}-(1-\mu\nabla^2)[k_W(w_b+w_s)-(k_P-N^T)\nabla^2(w_b+w_s)]=0.$$

3. Solution procedure

In this chapter, Galerkin's approach has been utilized for solving the non-local governing equations for thermal stability of a FGM nano-size plate having simply-supported (SSSS) and clamped (CCCC) edges as follows (Sobhy 2013):

Simply-supported (S)

$$\begin{aligned} &w_b=w_s=N_x=M_x^b=M_x^s=0 \quad \text{at} \quad x=0,a,\\ &w_b=w_s=N_y=M_y^b=M_y^s=0 \quad \text{at} \quad y=0,b. \end{aligned} \quad (35)$$

Clamped (C)

$$u=v=w_b=w_s=0 \quad \text{at} \quad x=0,a \quad \text{and} \quad y=0,b. \quad (36)$$

Four displacement components have been defined in below forms satisfying above conditions

$$u=\sum_{m=1}^{\infty}\sum_{n=1}^{\infty}\bar{A}_{mn}\bar{\Omega}_{mn}(x,y), \quad (37)$$

$$v=\sum_{m=1}^{\infty}\sum_{n=1}^{\infty}\bar{B}_{mn}\bar{\Phi}_{mn}(x,y), \quad (38)$$

$$w_b=\sum_{m=1}^{\infty}\sum_{n=1}^{\infty}\bar{C}_{mn}\bar{\Psi}_{mn}(x,y), \quad (39)$$

$$w_s=\sum_{m=1}^{\infty}\sum_{n=1}^{\infty}\bar{D}_{mn}\bar{\Psi}_{mn}(x,y), \quad (40)$$

where $\bar{A}_{mn}$, $\bar{B}_{mn}$, $\bar{C}_{mn}$ and $\bar{D}_{mn}$ are the unknown coefficients and $\bar{\Omega}_{mn}$, $\bar{\Phi}_{mn}$, $\bar{\Psi}_{mn}$ and $\bar{Y}_{mn}$ are admissible functions which are expressed as

Table 1 The admissible functions $X_m(x)$ and $Y_n(y)$ (Sobhy 2013)

Edge conditions			The functions X_m and Y_n	
	At $x=0,a$	At $y=0,b$	$X_m(x)$	$Y_n(y)$
SSSS	$X_m(0)=X_m''(0)=0$	$Y_n(0)=Y_n''(0)=0$	$\sin(\mathrm{m}\pi\mathrm{x}/\mathrm{a})$	$\sin(n\pi y/b)$
	$X_m(a)=X_m''(a)=0$	$Y_n(b)=Y_n''(b)=0$		
CCCC	$X_m(0)=X_m'(0)=0$	$Y_n(0)=Y_n'(0)=0$	$\sin^2(m\pi x/a)$	$\sin^2(n\pi y/b)$
	$X_m(a)=X_m'(a)=0$	$Y_n(b)=Y_n'(b)=0$		

$$\bar{\Omega}_{mn}(x,y)=\frac{\partial X_m(x)}{\partial x}Y_n(y), \quad (41)$$

$$\bar{\Phi}_{mn}(x,y)=X_m(x)\frac{\partial Y_n(y)}{\partial y}, \quad (42)$$

$$\bar{\Psi}_{mn}(x,y)=X_m(x)Y_n(y), \quad (43)$$

where two functions X_m and Y_n have been represented in Table 1 for considered edge conditions. Placing Eqs. (37)-(40) into Eqs. (31)-(34) gives

$$\begin{bmatrix} K_{1,1} & K_{1,2} & K_{1,3} & K_{1,4} \\ & K_{2,2} & K_{2,3} & K_{2,4} \\ & & K_{3,3} & K_{3,4} \\ sym. & & & K_{4,4} \end{bmatrix} \begin{Bmatrix} \bar{A}_{mn} \\ \bar{B}_{mn} \\ \bar{C}_{mn} \\ \bar{D}_{mn} \end{Bmatrix} = \{0\} \quad (44)$$

where

$$K_{1,1}=A_{11}\kappa_{12}+A_{66}\kappa_8, \quad K_{1,2}=(A_{12}+A_{66})\kappa_8, \quad K_{1,3}=-B_{11}\kappa_{12}-(B_{12}+2B_{66})\kappa_8, \quad (45)$$

$$K_{1,4}=-B_{11}^{s}\kappa_{12}-(B_{12}^{s}+2B_{66}^{s})\kappa_8, \quad K_{2,2}=A_{22}\kappa_4+A_{66}\kappa_{10},$$

$$K_{2,3}=-B_{22}\kappa_4-(B_{12}+2B_{66})\kappa_{10}, \quad K_{2,4}=-B_{22}^{s}\kappa_4-(B_{12}^{s}+2B_{66}^{s})\kappa_{10},$$

$$K_{3,3}=-D_{11}\kappa_{13}-2(D_{12}+2D_{66})\kappa_{11}-D_{22}\kappa_5-k_W\kappa_1-(\mu k_W-k_P+N^T)(\kappa_3+\kappa_9)+\mu(N^T-k_P)(\kappa_5+\kappa_{13}+2\kappa_{11}),$$

$$K_{3,4}=-D_{11}^{s}\kappa_{13}-2(D_{12}^{s}+2D_{66}^{s})\kappa_{11}-D_{22}^{s}\kappa_5-k_W\kappa_1-(\mu k_W-k_P+N^T)(\kappa_3+\kappa_9)+\mu(N^T-k_P)(\kappa_5+\kappa_{13}+2\kappa_{11}),$$

$$K_{4,4}=-H_{11}^{s}\kappa_{13}-2(H_{12}^{s}+2H_{66}^{s})\kappa_{11}-H_{22}^{s}\kappa_5+A_{44}^{s}\kappa_9+A_{55}^{s}\kappa_3-K_W\kappa_1-(\mu k_W-k_P+N^T)(\kappa_3+\kappa_9)+\mu(N^T-k_P)(\kappa_5+\kappa_{13}+2\kappa_{11})$$

in which

$$\begin{aligned}
\{\kappa_1,\kappa_3,\kappa_5\} &= \int_0^b\int_0^a \{X_mY_n, X_mY_n'', X_mY_n''''\}X_mY_n \mathrm{d}x\mathrm{d}y,\\
\{\kappa_9,\kappa_{11},\kappa_{13}\} &= \int_0^b\int_0^a \{X_m''Y_n, X_m''Y_n'', X_m''''Y_n\}X_mY_n \mathrm{d}x\mathrm{d}y,\\
\{\kappa_6,\kappa_8,\kappa_{12}\} &= \int_0^b\int_0^a \{X_m'Y_n, X_m'Y_n'', X_m'''Y_n\}X_m'Y_n \mathrm{d}x\mathrm{d}y,\\
\{\kappa_2,\kappa_4,\kappa_{10}\} &= \int_0^b\int_0^a \{X_mY_n', X_mY_n''', X_m''Y_n'\}X_mY_n' \mathrm{d}x\mathrm{d}y.
\end{aligned} \tag{46}$$

4. Types of thermal loading

There are three types of thermal loading considered in the present paper. The temperature field (T) for these loads can be expressed as (Javaheri and Eslami 2002)

Uniform temperature rise (UTR): $T = \Delta T + T_0$

Linear temperature rise (LTR): $T = T_m + \Delta T\left(\frac{1}{2}+\frac{z}{h}\right)$

Non-linear temperature rise (NLTR): $T = T_m + \Delta T\left(\frac{1}{2}+\frac{z}{h}\right)^{\beta}$

where β is the parameter of nonlinear temperature distribution. Here, T_0 defines the reference temperature. T_m defines the temperature of metal phase.

5. Discussions on obtained results

The present section is devoted to provide a variety of numerical findings to investigate the thermal buckling characteristics of a fully clamped E-FGM nanoplate employing 4-unknown refined theory. The elastic properties of both metal and ceramic materials are represented in Table 2. To ensure the validity of the present shear deformation theory in predicting thermal buckling behavior of FGM plates, the obtained results are compared with the existing ones in the literature. A comparison between buckling results for a simply-supported FG plate under uniform and linear temperature rises based on presented theory and those of Bouhadra *et al.* (2015) is presented in Table 3 and a good agreement is observed. Also, critical buckling temperatures of present study for a clamped FG plate are compared with those of Bateni *et al*. (2013) and Bouhadra *et al*. (2015) and the results are represented in Table 4. One can found that the critical buckling temperatures predicted via shear deformation theories are identical. However, CPT which ignores shear deformation effect provides larger critical temperatures. Next, for better representation of the obtained results the below normalized factors have been defined

$$K_W = \frac{k_W a^4}{D_c}, \qquad K_P = \frac{k_p a^2}{D_c}, \qquad D_c = \frac{E_c h^3}{12(1-\nu_c^2)}. \tag{47}$$

The effects of different values of non-local factor (μ), gradient index (p) and length-to-thickness ratio (a/h) on critical buckling temperature of clamped E-FGM nanoplate resting on elastic foundation accounting for uniformly-type, linearly-type and non-linearly temperature rises is represented in Tables 5-7, respectively. It can be deduced that for all types of thermal loadings, nonlocality has a decreasing influence on structural plate stiffness and critical buckling temperatures of clamped E-FGM nanoplates. Also, presence of elastic foundation increases the plate stiffness as well as critical buckling temperatures. Moreover, one may observe that for every value of non-local factor and all types of thermal loadings increasing in side-to-thickness ratio (a/h) reduces the critical temperature (ΔT_{cr}). Also, it is worth mentioning that at a prescribed contact condition, non-linear temperature rise (NLTR) provides greater critical temperature than uniformly (UTR) and linearly temperature rises (LTR) for a clamped FGM nanoplate.

Table 2 Material properties for metal and ceramic constituents

Property	Metallic	Ceramic
E (GPa)	70	380
α ($1/K$)	23e-6	7.4e-6
ν	0.3	0.3

Table 3 Critical buckling temperatures for SSSS FGM plate based on different shear deformation plate theories ($a/h = 100$)

p	Theory	Uniform			Linear		
		$a/b=1$	$a/b=2$	$a/b=3$	$a/b=1$	$a/b=2$	$a/b=3$
0	Present	17.0895	42.6876	85.2551	24.1789	75.3752	160.510
	HPT	17.0894	42.6876	85.2553	24.1789	75.3752	160.510
	SPT	17.0894	42.6876	85.2554	24.1789	75.3753	160.510
	TPT	17.0894	42.6875	85.2551	24.1789	75.3751	160.510
	CPT	17.0991	42.7477	85.4955	24.1982	75.4955	160.991
1	Present	7.94001	19.8359	39.6248	5.51388	27.8242	64.937
	HPT	7.94000	19.8359	39.6248	5.5138	27.8242	64.937
	SPT	7.94000	19.8359	39.6249	5.5138	27.8242	64.937
	TPT	7.94000	19.8358	39.6248	5.5138	27.8242	64.937
	CPT	7.94370	19.8594	39.7188	5.5209	27.8683	65.114
5	Present	7.26066	18.1327	36.2025	3.89125	22.6052	53.708
	HPT	7.2607	18.1330	36.2037	3.8913	22.6057	53.710
	SPT	7.2606	18.1324	36.2014	3.8911	22.6047	53.706
	TPT	7.2606	18.1327	36.2025	3.8912	22.6052	53.708
	CPT	7.2657	18.1642	36.3285	3.8999	22.6595	53.925

Table 4 Comparisons of critical buckling temperatures for square clamped P-FGM plates for various material compositions

a/h	Theory	Gradient exponent (p)				
		0	0.5	1	2	5
50	Present	181.31	102.795	84.3067	74.7146	76.9296
	Bouhadra *et al.* (2015)	181.3	102.795	84.307	74.715	76.934
	Bateni *et al.* (2013)	180.3	102.23	83.84	74.3	76.5
100	Present	45.5291	25.8004	21.1566	18.7548	19.3393
	Bouhadra *et al.* (2015)	45.529	25.8	21.156	18.754	19.339
	Bateni *et al.* (2013)	45.28	25.65	21.04	18.65	19.23

Table 5 Critical buckling temperatures for CCCC E-FGM nanoplates rested on elastic substrate with uniform temperature rise

μ	(K_W, K_P)	$a/h = 5$		$a/h = 10$		
		$p = 0.5$	$p = 1$	$p = 2$	$p = 1$	$p = 2$
0	(0,0)	6477.69	5608.72	2574.44	2199.56	1975.1
	(50,0)	7336.48	6549.88	2770.96	2414.26	2210.39
	(50,10)	11857	11503.9	3805.43	3544.38	3448.91
1	(0,0)	4243.83	3674.53	1686.63	1441.03	1293.98
	(50,0)	4954.54	4453.41	1849.27	1618.71	1488.7
	(50,10)	9475.03	9407.47	2883.74	2748.83	2727.22
2	(0,0)	3155.6	2732.29	1254.14	1071.52	962.171
	(50,0)	3794.18	3432.11	1400.27	1231.16	1137.13
	(50,10)	8314.67	8386.17	2434.74	2361.28	2375.64

Table 6 Critical buckling temperatures for CCCC E-FGM nanoplates rested on elastic substrate with linear temperature rise

μ	$(K_W, K_P$	$a/h = 5$			$a/h = 10$		
		$p = 0.5$	$p = 1$	$p = 2$	$p = 0.5$	$p = 1$	$p = 2$
0	(0,0)	14254.8	11849.7	10226.6	4791.68	4017.64	3595.37
	(50,0)	15720.7	13421.9	11944.2	5158.17	4410.69	4024.76
	(50,10)	23437.4	21697.6	20985.1	7087.33	6479.63	6285
1	(0,0)	9335.73	7760.11	6696.75	3136.03	2628.98	2352.34
	(50,0)	10548.9	9061.22	8118.17	3439.33	2954.26	2707.7
	(50,10)	18265.6	17337	17159.2	5368.49	5023.2	4967.94
2	(0,0)	6939.42	5767.88	4977.2	2329.48	1952.49	1746.8
	(50,0)	8029.49	6936.93	6254.35	2602	2244.76	2066.09
	(50,10)	15746.1	15212.7	15295.3	4531.15	4313.7	4326.33

Table 7 Critical buckling temperatures for CCCC E-FGM nanoplates rested on elastic substrate with non-linear temperature rise

μ	$\left(\frac{K_W}{,K_P}\right)$	$a/h = 5$			$a/h = 10$		
0	(0,0)	$p = 0.5$	$p = 1$	$p = 2$	$p = 0.5$	$p = 1$	$p = 2$
	(0,0)	27199.2	22098.2	18722.0	9142.9	7492.39	6582.11
	(50, 0)	29996.4	25030.1	21866.4	9842.2	8225.38	7368.22
	(50, 10)	44720.4	40463.4	38418.0	13523.2	12083.7	11506.1
1	(0,0)	17813.3	14471.6	12259.9	5983.79	4902.71	4306.48
	(50, 0)	20128.2	16898.0	14862.1	6562.52	5509.32	4957.04
	(50, 10)	34852.1	32331.3	31413.6	10243.5	9367.63	9094.92
2	(0,0)	13241	10756.4	9111.86	4444.84	3641.16	3197.91
	(50, 0)	15320.9	12936.5	11450.0	4964.82	4186.19	3782.43
	(50, 10)	30044.8	28369.7	28001.5	8645.8	8044.5	7920.31

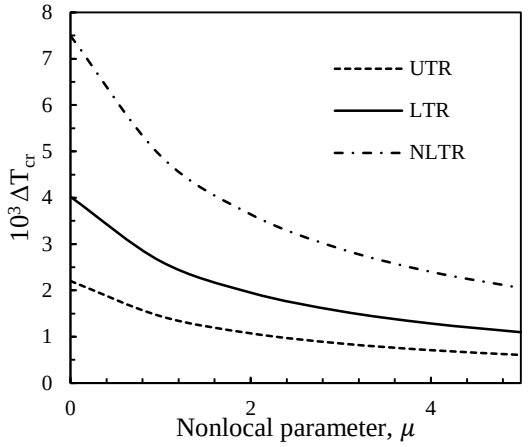

Fig. 2 Variations of critical buckling temperatures of clamped FGM nanoplate subjected to different temperature rises versus nonlocal parameter ($a = b = 10h,\ K_W = K_P = 0$)

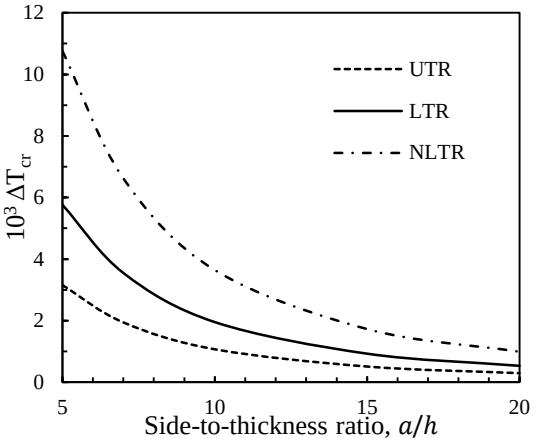

Fig. 3 Variations of critical buckling temperatures of clamped FGM nano-size plate with respect to length-to-thickness ratio subjected to different temperature rises ($p = 1,\ \mu = 2\ \text{nm}^2,\ K_W = K_P = 0$)

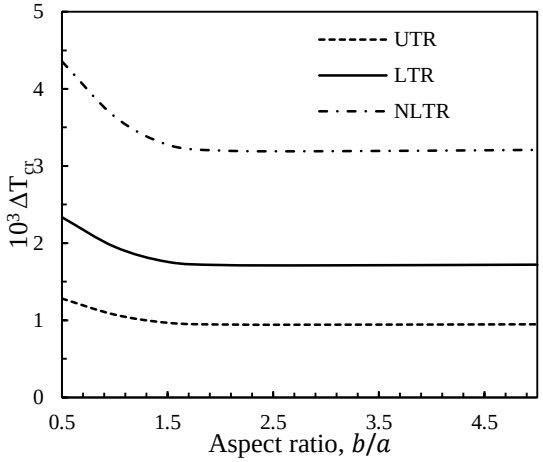

Fig. 4 4 Variations of critical buckling temperatures of clamped FGM nano-size plate with respect to aspect ratio based on different thermal loads ($a/h = 10,\ p = 1,\ \mu = 2\ \text{nm}^2,\ K_W = K_P = 0$)

The critical buckling temperatures as functions of nonlocal parameter for a E-FG nanoplate with clamped edge conditions under different thermal loadings (UTR, LTR and NLTR) at length-to-thickness ratio $a/h = 10$ is depicted in Fig. 2. One can see that for all thermal loadings, a nonlocal clamped E-FG nanoplate has lower critical temperatures than local one. This is due to the fact that nonlocality makes the nanoplate structure less rigid. Moreover, it is found that the reduction in critical buckling temperatures of clamped E-FGM nano-size plate based upon NLTR is more considerable than UTR and LTR.

The variations of critical buckling temperatures of clamped E-FGM nano-size plate according to length-to-thickness ratio (a/h) based on different thermal loadings at $p = 1$, $K_W = K_P = 0$ and $\mu = 2\ \text{nm}^2$ is represented in Fig. 3. As previously stated, non-linear and uniformly temperature rises, respectively, provide largest and smallest values of critical temperature difference.

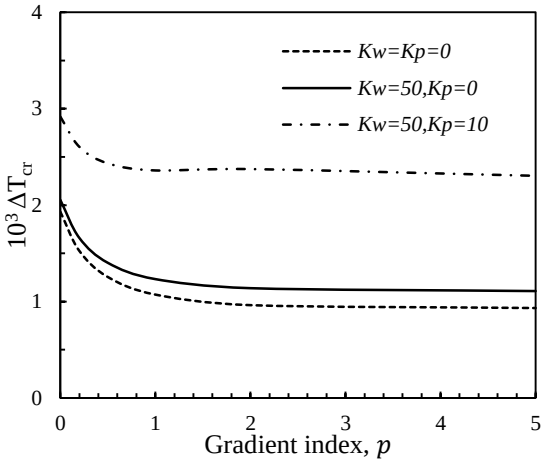

Fig. 5 Variations of critical buckling temperatures of clamped FGM nano-size plate rested on elastic substrate under uniformly temperature change versus gradient index ($a = b = 10h\ \ \mu = 2\ \text{nm}^2$)

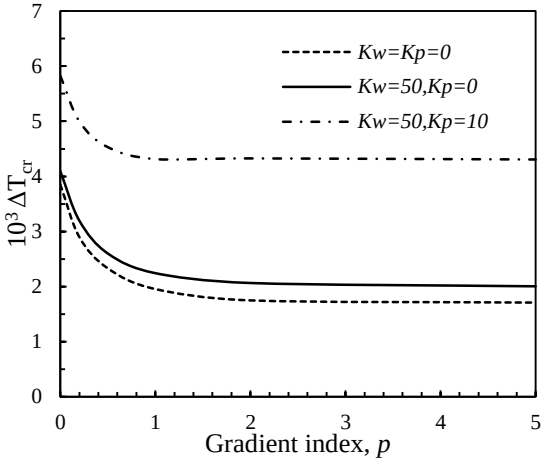

Fig. 6 Variations of critical buckling temperatures of clamped FGM nano-size plate rested on elastic substrate under linearly temperature change versus gradient index ($a = b = 10h\ \ \mu = 2\ \text{nm}^2$)

Another observation is that reduction in critical buckling temperature with respect to side-to-thickness ratio according to non-linear thermal loading ($\beta = 3$) is more considerable than uniform and linear thermal loads. Therefore, it can be deduced that stability behavior of a clamped E-FG nanoplate is affected considerably by the kind of thermal loading.

Influence of plate aspect ratio (b/a) on the critical buckling temperatures of clamped E-FGM nanoplates under different temperature fields at $a/h = 10$, $p = 1$, $K_W = K_P = 0$ and $\mu = 2$ nm^2 is presented in Fig. 4. It can be seen that critical buckling temperature reduces by increasing aspect ratio, especially for smaller values of plate aspect ratio (b/a).

Variation of critical buckling temperature of clamped E-FGM nanoplate with respect to gradient index for different values of elastic foundation parameters under uniform, linear and nonlinear temperature fields at $\mu = 2$ nm^2 is plotted in Figs. 5-7, respectively. It is observable that lower values of gradient index have more prominent reducing impact on the buckling response of clamped FG nanoplate, while higher gradient indexes show no significant effect on critical buckling temperatures. Furthermore, one can see that the Pasternak layer factor of the elastic substrate provides more prominent impacts on critical temperatures difference than Winkler factor. Hence, by increasing Pasternak factor (K_P) the critical buckling temperatures enhance considerably.

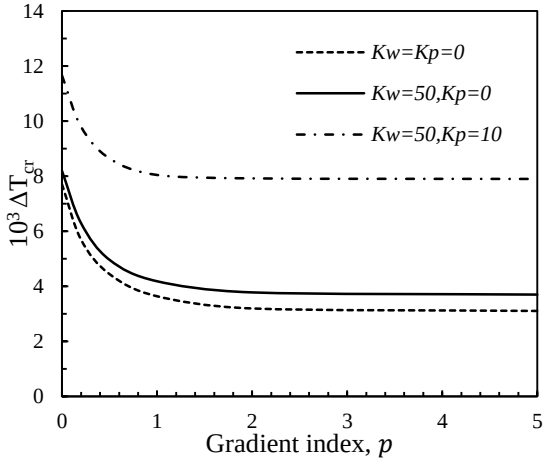

Fig. 7 Variations of critical buckling temperatures of clamped FGM nano-size plate rested on elastic substrate under non-linear temperature change versus gradient index ($a = b = 10h$ $\mu = 2$ nm^2)

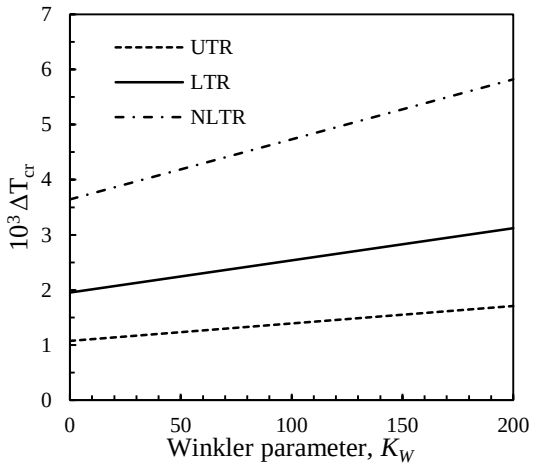

Fig. 8 Effects of Winkler factor on critical buckling temperatures of clamped FGM nano-size plate with different temperature changes ($a = b = 10h$ $\mu = 2$ nm^2)

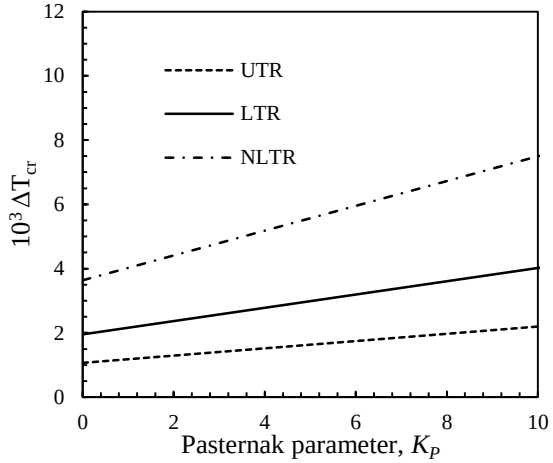

Fig. 9 Effects of Pasternak factor on critical buckling temperatures of clamped FGM nano-size plate under different temperature changes ($a = b = 10h$, $\mu = 2$ nm^2)

To show the effect of elastic substrate factors on thermal buckling behaviors of clamped E-FGM nano-size plate individually, Figs. 8 and 9 represent changing of the critical temperatures difference versus Winkler and Pasternak factors, respectively, at $a/h = 10$ and $\mu = 2$ nm^2. One may found from the figures that regardless of the kind of thermal field, the critical buckling temperatures arise by increasing of Winkler and Pasternak factors, due to the increment in stiffness of the FGM nano-size plate. However, according to the figures, it is evident that non-linearly temperature distribution (NLTR) gives greater value for ΔT_{cr} than UTR and LTR, while UTR gives the lower values for critical temperatures. Moreover, at larger values of elastic substrate parameter, the differences between the critical temperatures according to various thermal loadings become more prominent.

6. Conclusions

This article investigates thermal stability of clamped nano-size plates with exponentially graded material properties under uniform, linear and non-linear thermal loadings based on a secant function based refined plate theory. Hamilton's rule and non-local constitutive relations of Eringen are used to derive the non-local governing differential equations based on four-unknown plate formulation. These equations have been solved by applying

Galerkin's solution which captures clamped boundary conditions. It is indicated that thermal buckling response of clamped E-FGM nanoplate is affected by various parameters such as nonlocality, elastic foundation parameters, material graduation, thermal environments, and aspect and side-to-thickness ratios. It is observed that the nonlocality reduces the plate stiffness and critical buckling temperatures. Also, it is found that the Winkler and Pasternak parameters of elastic foundation increase the critical buckling temperatures. Moreover, it is concluded that smaller values of gradient index have more considerable effect on critical buckling temperature of E-FGM nanoplate than larger one. Also, it is observed that non-linear temperature distribution has greater critical buckling temperatures than uniformly and linearly temperature distributions.

Acknowledgements

The authors would like to thank Mustansiriyah university (www.uomustansiriyah.edu.iq) Baghdad-Iraq, for their support in the present work.

References

Abualnour, M., *et al.* (2018), "A novel quasi-3D trigonometric plate theory for free vibration analysis of advanced composite plates", *Compos. Struct*., **184**, 688-697.

Addou, F.Y., *et al.* (2019), "Influences of porosity on dynamic response of FG plates resting on Winkler/Pasternak/Kerr foundation using quasi 3D HSDT", *Comput. Concrete*, **24**(4),347-367. https://doi.org/10.12989/cac.2019.24.4.347.

Ahouel, M., Houari, M.S.A., Bedia, E.A. and Tounsi, A. (2016), "Size-dependent mechanical behavior of functionally graded trigonometric shear deformable nanobeams including neutral surface position concept", *Steel Compos. Struct.*, **20**(5), 963-981. https://doi.org/10.12989/scs.2016.20.5.963.

Akavci, S.S. (2014), "An efficient shear deformation theory for free vibration of functionally graded thick rectangular plates on elastic foundation", *Compos. Struct.*, **108**, 667-676. https://doi.org/10.1016/j.compstruct.2013.10.019.

Alimirzaei, S., *et al.* (2019), "Nonlinear analysis of viscoelastic micro-composite beam with geometrical imperfection using FEM: MSGT electro-magneto-elastic bending, buckling and vibration solutions", *Struct. Eng. Mech*., **71**(5), 485-502. https://doi.org/10.12989/scs.2019.71.5.485.

Al-Maliki, A.F., Faleh, N.M. and Alasadi, A.A. (2019), "Finite element formulation and vibration of nonlocal refined metal foam beams with symmetric and non-symmetric porosities", *Struct. Monit. Maint*., **6**(2), 147-159. https://doi.org/10.12989/smm.2019.6.2.147.

Atmane, H.A., Tounsi, A., Bernard, F. and Mahmoud, S.R. (2015), "A computational shear displacement model for vibrational analysis of functionally graded beams with porosities", *Steel Compos. Struct.*, **19**(2), 369-384. https://doi.org/10.12989/scs.2015.19.2.369.

Attia, A., *et al.* (2018), "A refined four variable plate theory for thermoelastic analysis of FGM plates resting on variable elastic foundations", *Struct. Eng. Mech*., 65(4), 453-464. https://doi.org/10.12989/scs.2018.65.4.453.

Aydogdu, M. (2009), "A general nonlocal beam theory: its application to nanobeam bending, buckling and vibration", *Phys. E*, **41**(9), 1651-1655. https://doi.org/10.1016/j.physe.2009.05.014.

Bakhadda, B., *et al*. (2018), "Dynamic and bending analysis of carbon nanotube-reinforced composite plates with elastic foundation", *Wind Struct*., **27**(5), 311-324. https://doi.org/10.12989/was.2018.27.5.311.

Bateni, M., Kiani, Y. and Eslami, M.R. (2013), "A comprehensive study on stability of FGM plates", *Int. J. Mech. Sci.*, **75**, 134-144. https://doi.org/10.1016/j.ijmecsci.2013.05.014.

Beldjelili, Y., *et al.* (2016), "Hygro-thermo-mechanical bending of S-FGM plates resting on variable elastic foundations using a four-variable trigonometric plate theory", *Smart Struct. Syst*., **18**(4), 755-786. https://doi.org/10.12989/sss.2016.18.4.755.

Berghouti, H., *et al*. (2019), "Vibration analysis of nonlocal porous nanobeams made of functionally graded material", *Adv. Nano Res.*, **7**(5), 351-364. https://doi.org/10.12989/anr.2019.7.5.351.

Besseghier, A., Heireche, H., Bousahla, A.A., Tounsi, A. and Benzair, A. (2015), "Nonlinear vibration properties of a zigzag single-walled carbon nanotube embedded in a polymer matrix", *Adv. Nano Res.,* **3**(1), 29-37. https://doi.org/10.12989/anr.2015.3.1.029.

Bouhadra, A., Benyoucef, S., Tounsi, A., Bernard, F., Bouiadjra, R. B. and Sid Ahmed Houari, M. (2015), "Thermal buckling response of functionally graded plates with clamped boundary conditions", *J. Therm. Stress.*, **38**(6), 630-650. https://doi.org/10.1080/01495739.2015.1015900.

Boukhlif, Z., *et al.* (2019), "A simple quasi-3D HSDT for the dynamics analysis of FG thick plate on elastic foundation", *Steel Compos. Struct*., **31**(5), 503-516. https://doi.org/10.12989/scs.2019.31.5.503.

Boulefrakh et al. (2019), "The effect of parameters of visco-Pasternak foundation on the bending and vibration properties of a thick FG plate", *Geomech. Eng*., **18**(2), 161-178. https://doi.org/10.12989/gae.2019.18.2.161.

Bounouara, F., *et al.* (2016), "A nonlocal zeroth-order shear deformation theory for free vibration of functionally graded nanoscale plates resting on elastic foundation", *Steel Compos. Struct*., **20**(2), 227-249. https://doi.org/10.12989/scs.2016.20.2.227.

Bourada, F., *et al.* (2019), "Dynamic investigation of porous functionally graded beam using a sinusoidal shear deformation theory", *Wind Struct*., **28**(1), 19-30. https://doi.org/10.12989/was.2019.28.1.019.

Boutaleb, S., *et al.* (2019), "Dynamic Analysis of nanosize FG rectangular plates based on simple nonlocal quasi 3D HSDT", *Adv. Nano Res*,, **7**(3), 189-206. https://doi.org/10.12989/anr.2019.7.3.189.

Chaabane, L.A., *et al.* (2019), "Analytical study of bending and free vibration responses of functionally graded beams resting on elastic foundation", *Struct. Eng. Mech*., **71**(2), 185-196. https://doi.org/10.12989/sem.2019.71.2.185.

Chemi, A., Heireche, H., Zidour, M., Rakrak, K. and Bousahla, A.A. (2015), "Critical buckling load of chiral double-walled carbon nanotube using non-local theory elasticity", *Adv. Nano Res*., **3**(4), 193-206. https://doi.org/10.12989/anr.2015.3.4.193.

Draiche, K., *et al.* (2019), "Static analysis of laminated reinforced composite plates using a simple first-order shear deformation theory", *Comput. Concrete*, **24**(4), 369-378. https://doi.org/10.12989/cac.2019.24.4.369.

Ebrahimi, F. and Barati, M.R. (2015), "A Nonlocal Higher-Order Shear Deformation Beam Theory for Vibration Analysis of Size-Dependent Functionally Graded Nanobeams", *Arab. J. Sci. Eng.*, 1-12. https://doi.org/10.1007/s13369-015-1930-4.

El-Haina, F., *et al*. (2017), "A simple analytical approach for thermal buckling of thick functionally graded sandwich plates", *Struct. Eng. Mech*., **63**(5), 585-595. https://doi.org/10.12989/sem.2017.63.5.585.

Eringen, A.C. and Edelen, D.G.B. (1972), "On nonlocal elasticity", *Int. J. Eng. Sci.*, **10**(3), 233-248. https://doi.org/10.1016/0020-7225(72)90039-0.

Eringen, A.C. (1983), "On differential equations of nonlocal elasticity and solutions of screw dislocation and surface waves", *J. Appl. Phys.*, **54**(9), 4703-4710. https://doi.org/10.1063/1.332803.

Fenjan, R.M., Ahmed, R.A., Alasadi, A.A. and Faleh, N.M. (2019), "Nonlocal strain gradient thermal vibration analysis of double-coupled metal foam plate system with uniform and non-uniform porosities", *Coupled Syst. Mech.*, **8**(3), 247-257.

Hamza-Cherif, R., *et al.* (2018), "Vibration analysis of nano beam using differential transform method including thermal effect", *J. Nano Res.*, **54**, 1-14.

Houari, M.S.A., Bessaim, A., Bernard, F., Tounsi, A. and Mahmoud, S.R. (2018), "Buckling analysis of new quasi-3D FG nanobeams based on nonlocal strain gradient elasticity theory and variable length scale parameter", *Steel Compos. Struct.*, **28**(1), 13-24. https://dx.doi.org/10.12989/scs.2018.28.1.013.

Kettaf, F.Z., Houari, M.S.A., Benguediab, M. and Tounsi, A. (2013), "Thermal buckling of functionally graded sandwich plates using a new hyperbolic shear displacement model", *Steel Compos. Struct.*, **15**(4), 39. http://dx.doi.org/10.12989/scs.2013.15.4.399.

Mahi, A. and Tounsi, A. (2015), "A new hyperbolic shear deformation theory for bending and free vibration analysis of isotropic, functionally graded, sandwich and laminated composite plates", *Appl. Math. Model.*, **39**(9), 2489-2508. https://doi.org/10.1016/j.apm.2014.10.045.

Mahmoudi, A., *et al.* (2019), "A refined quasi-3D shear deformation theory for thermo-mechanical behavior of functionally graded sandwich plates on elastic foundations", *J. Sandw. Struct. Mater.*, **21**(6), 1906-1926.

Mantari, J.L., Oktem, A.S. and Soares, C.G. (2012), "A new trigonometric shear deformation theory for isotropic, laminated composite and sandwich plates", *Int. J. Solid. Struct.*, **49**(1), 43-53.

Menasria, A., *et al.* (2017), "A new and simple HSDT for thermal stability analysis of FG sandwich plates", *Steel Compos. Struct.*, **25**(2), 157-175. http://dx.doi.org/10.12989/scs.2017.25.2.157.

Mirjavadi, S.S., Afshari, B.M., Shafiei, N., Hamouda, A.M.S. and Kazemi, M. (2017), "Thermal vibration of two-dimensional functionally graded (2D-FG) porous Timoshenko nanobeams," *Steel Compos. Struct.*, **25**(4), 415-426. https://doi.org/10.12989/scs.2017.25.4.415.

Mokhtar, Y., *et al.* (2018), "A novel shear deformation theory for buckling analysis of single layer graphene sheet based on nonlocal elasticity theory", *Smart Struct. Syst.*, **21**(4), 397-405. https://doi.org/10.12989/sss.2018.21.4.397.

Murmu, T. and Adhikari, S. (2010), "Nonlocal transverse vibration of double-nanobeam-systems", *J. Appl. Phys.*, **108**(8), 083514. https://doi.org/10.1063/1.3496627.

Natarajan, S., Chakraborty, S., Thangavel, M., Bordas, S. and Rabczuk, T. (2012), "Size-dependent free flexural vibration behavior of functionally graded nanoplates", *Comput. Mat. Sci.*, **65**, 74-80. https://doi.org/10.1016/j.commatsci.2012.06.031.

Nguyen, V.H., Nguyen, T.K., Thai, H.T. and Vo, T.P. (2014), "A new inverse trigonometric shear deformation theory for isotropic and functionally graded sandwich plates", *Compos. B*, **66**, 233-246. https://doi.org/10.1016/j.compositesb.2014.05.012.

Oktem, A.S., Mantari, J.L. and Soares, C.G. (2012), "Static response of functionally graded plates and doubly-curved shells based on a higher order shear deformation theory", *Eur. J. Mech. A/Solid.*, **36**, 163-172. https://doi.org/10.1016/j.euromechsol.2012.03.002.

Pradhan, S.C. and Phadikar, J.K. (2009), "Nonlocal elasticity theory for vibration of nanoplates", *J. Sound. Vib.*, **325**(1), 206-223. https://doi.org/10.1016/j.jsv.2009.03.007.

Reddy, J.N. (1984), "A simple higher-order theory for laminated composite plates", *J. Appl. Mech.*, **51**(4), 745-752. https://doi.org/10.1115/1.3167719.

Reddy, J.N. (2007), "Nonlocal theories for bending, buckling and vibration of beams", *Int. J. Eng. Sci.*, **45**(2), 288-307. https://doi.org/10.1016/j.ijengsci.2007.04.004.

Sahoo, R. and Singh, B.N. (2013), "A new inverse hyperbolic zigzag theory for the static analysis of laminated composite and sandwich plates", *Compos. Struct.*, **105**, 385-397. https://doi.org/10.1016/j.compstruct.2013.05.043.

Semmah, A., *et al.* (2019), "Thermal buckling analysis of SWBNNT on Winkler foundation by non local FSDT", *Adv. Nano Res.*, **7**(2), 89-98. https://doi.org/10.12989/anr.2019.7.2.089.

Sobhy, M. (2013), "Buckling and free vibration of exponentially graded sandwich plates resting on elastic foundations under various boundary conditions", *Compos. Struct.*, **99**, 76-87. https://doi.org/10.1016/j.compstruct.2012.11.018.

Soldatos, K.P. (1992), "A transverse shear deformation theory for homogeneous monoclinic plates", *Acta Mech.*, **94**(3-4), 195-220. https://doi.org/10.1007/BF01176650.

Taj, M.G., Chakrabarti, A. and Sheikh, A.H. (2013), "Analysis of functionally graded plates using higher order shear deformation theory", *Appl. Math. Model.*, **37**(18), 8484-8494. https://doi.org/10.1016/j.apm.2013.03.058.

Thai, C.H., Ferreira, A.J.M., Bordas, S.P.A., Rabczuk, T. and Nguyen-Xuan, H. (2014), "Isogeometric analysis of laminated composite and sandwich plates using a new inverse trigonometric shear deformation theory", *Eur. J. Mech. A-Solid.*, **43**, 89-108. https://doi.org/10.1016/j.euromechsol.2013.09.001.

Tlidji, Y., *et al.* (2019), "Vibration analysis of different material distributions of functionally graded microbeam", *Struct. Eng. Mech.*, **69**(6), 637-649. https://doi.org/10.12989/sem.2019.69.6.637.

Youcef, D.O., *et al.* (2018), "Dynamic analysis of nanoscale beams including surface stress effects", *Smart Struct. Syst.*, **21**(1), 65-74. https://doi.org/10.12989/sss.2018.21.1.065.

Zarga, D., *et al.* (2019), "Thermomechanical bending study for functionally graded sandwich plates using a simple quasi-3D shear deformation theory", *Steel Compos. Struct.*, **32**(3), 389-410. https://doi.org/10.12989/scs.2019.32.3.389.

CC